Journal of Digital Imaging

Information Entropy Measure for Evaluation of Image Quality

Du-Yih Tsai,[1] Yongbum Lee,[1] and Eri Matsuyama[2]

This paper presents a simple and straightforward method for synthetically evaluating digital radiographic images by a single parameter in terms of transmitted information (TI). The features of our proposed method are (1) simplicity of computation, (2) simplicity of experimentation, and (3) combined assessment of image noise and resolution (blur). Two acrylic step wedges with 0–1–2–3–4–5 and 0–2–4–6–8–10 mm in thickness were used as phantoms for experiments. In the present study, three experiments were conducted. First, to investigate the relation between the value of TI and image noise, various radiation doses by changing exposure time were employed. Second, we examined the relation between the value of TI and image blurring by shifting the phantoms away from the center of the X-ray beam area toward the cathode end when imaging was performed. Third, we analyzed the combined effect of deteriorated blur and noise on the images by employing three smoothing filters. Experimental results show that the amount of TI is closely related to both image noise and image blurring. The results demonstrate the usefulness of our method for evaluation of physical image quality in medical imaging.

KEY WORDS: Medical images, image quality, image processing, information entropy, performance evaluation

INTRODUCTION

In medical imaging, image quality is determined by at least five factors: contrast, resolution, noise, artifacts, and distortion. Of these factors, resolution and noise are the most commonly used physical characteristics. As is well known, they are described by the modulation transfer function (MTF) and noise power spectrum (NPS), respectively. The MTF describes the ability of an imaging system to reproduce the frequency information contained in the incident X-ray signal. The NPS describes the frequency content of the noise of an imaging system. However, one of the dilemmas in medical radiography is the extent to which these metrics affect image quality. In comparison of two imaging systems, for example, an imaging system may only be superior in one metric while being inferior to another in the other metric. To deal with this issue, the noise equivalent quanta or detective quantum efficiency, which can be calculated if the MTF, NPS, and the input signal-to-noise ratio of the X-ray beam used to measure the NPS are known, is used as a single parameter to describe the general quality of the system.[1,2]

In this study, we present a simple and straightforward method for synthetically evaluating digital radiographic images by a single parameter in terms of Shannon's entropy (information entropy).[3,4] Our proposed method is considered as an alternative to the currently available metrics for evaluation of image quality. The concept of information entropy describes how much randomness (or uncertainty) there is in a signal or an image; in other words, how much information is

[1]*From the Department of Radiological Technology, School of Health Sciences, Niigata University, 2-746, Asahimachi-dori, Niigata, 951-8518, Japan.*

[2]*From the Department of Radiological Technology, Graduate School of Health Sciences, Niigata University, 2-746, Asahimachi-dori, Niigata, 951-8518, Japan.*

Correspondence to: Du-Yih Tsai, Ph.D., Department of Radiological Technology, School of Health Sciences, Niigita University, 2-746, Asahimachi-dori, Niigata, 951-8518, Japan; tel: +81-25-2270965; fax: +81-25-2270749; e-mail: tsai@clg.niigata-u.ac.jp

Online publication 19 June 2007

doi: 10.1007/s10278-007-9044-5

provided by the signal or image. If the uncertainty is measured before and after imaging, the reduction in the uncertainty, i.e., information entropy is a quantitative measure of the information transmitted by the image. The image quality then can be quantitatively compared when the transmitted information (TI) provided by the images are known. From the physical measurement's point of view, the more information is transmitted, the better the image quality is.

To the best of our knowledge, the research that initially led to the introduction of TI as an image quality measure dates back to the late 1970s. Uchida and Tsai first introduced a method in terms of entropy for quality evaluation of radiographic images and applied this method to assess the quality of tank-developed images and that of automatic processor-developed images.[5] They demonstrated that the quality of radiographic images were largely affected by the characteristics of X-ray apparatus, exposure factors, intensifying screen-film system, and film development process. If all of these parameters affecting the image quality are kept unvaried, except the film development method, the performance of development methods can be quantitatively assessed by comparing the amounts of information contributed by tank-developed images and automatic processor-developed images. After this publication, limited work using the TI as an image quality measure for image assessment has been reported,[6,7] although a great deal of work on mutual-information-based registration of monomodality and multimodality medical images has been devoted since the early 1990s.[8–17]

The present paper is a significant extension of our previous work,[5] applying the methodology to the field of digital medical imaging. The features of our proposed method are (1) simplicity of computation, (2) simplicity of experimentation, and (3) combined assessment of noise and resolution (blur) by a single number. In this study, to validate the usefulness of our proposed method, three experiments were given.

THEORETICAL FRAMEWORK

TI is a concept from information theory. We briefly describe the TI as follows.

Given events S_1,..., S_n occurring with probabilities $p(S_1)$, ..., $p(S_n)$, then the average uncertainty associated with each event is defined by the Shannon entropy as

$$H(S) = -\sum_{i=1}^{n} p(S_i) \cdot \log_2 p(S_i), \qquad (1)$$

Considering x and y as two random variables corresponding to an input variable and an output variable, the entropy for the input and that for the output are denoted as $H(x)$ and $H(y)$, respectively. For this case the joint entropy, $H(x, y)$, is defined as

$$H(x,y) = H(x) + H_x(y) = H(y) + H_y(x) \qquad (2)$$

where $H_x(y)$ and $H_y(x)$ are conditional entropies. They are the entropy of the output when the input is known and that of the input when the output is known, respectively. In this situation, we can compute TI, $T(x; y)$, as:

$$\begin{aligned} T(x;y) &= H(x) - H_y(x) = H(y) - H_x(y) \\ &= H(x) + H(y) - H(x,y). \end{aligned} \qquad (3)$$

A useful way of visualizing the relationship between these entropies is provided by a Venn diagram as shown in Figure 1. Consider an experiment in which every input has a unique output belonging to one of various output categories. In this study, for simplicity, the inputs may be considered to be a set of subjects (e.g., phantoms in simplicity) varying in composition, while the outputs may be their corresponding images varying in optical density or gray level. An orderly system firstly established by Attneave[18] is employed in the present study to calculate the entropies of input, output, and their joint entropies. With this orderly system, the amount of TI is easily computed. The frequency with which each output is made to each input is recorded in Table 1. The columns and rows of this table represent various inputs and outputs. The various inputs, x_1, x_2, ..., x_i, ..., X, are assumed to take discrete values of input variables x. Likewise, the various outputs, y_1, y_2, ..., y_j, Y, are discrete values of output variables y. The upper-case X and Y stand for the number of input and output categories, respectively. Note that the subscript i refers to any particular but unspecified input, whereas the subscript j refers to any particular but unspeci-

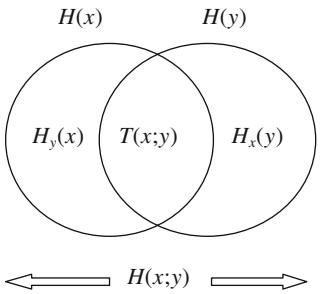

Fig 1. Venn diagram that represents the relationship between input entropy *H*(*x*) and output entropy *H*(*y*), conditional entropies $H_x(y)$, and $H_y(x)$, joint entropy *H*(*x*, *y*), and the transmitted information *T*(*x*; *y*). The amount of each entropy and transmitted information are shown by each area in the diagram.

fied output. The number of times input x_i is presented will be symbolized by n_i, the frequency of output, y_j, by n_j, and the frequency, with which the input x_i corresponds to the output y_j, is given by n_{ij}. The total of all frequencies is given by n. It is apparent from Table 1 that

$$\sum_j n_{ij} = n_i \tag{4}$$

$$\sum_i n_{ij} = n_j \tag{5}$$

$$\sum_{ij} n_{ij} = \sum_i n_i = \sum_j n_j = n \quad . \tag{6}$$

Referring to the definition of information entropy as shown in Eq. 1, three informational

Table 1. A Data Matrix of Frequency for *Y* Outputs to *X* Inputs

n_{11}	n_{21}	–	n_{i1}	–	–	n_{X1}
n_{12}	n_{22}	–	n_{i2}	–	–	n_{X2}
n_{13}	n_{23}	–	n_{i3}	–	–	n_{X3}
–	–	–	–	–	–	–
n_{1j}	n_{2j}	–	n_{ij}	–	–	n_{Xj}
–	–	–	–	–	–	–
n_{1Y}	n_{2Y}	–	n_{iY}	–	–	n_{XY}

The columns and rows of this table represent various discrete inputs and outputs. The capitals *X* and *Y* stand for the number of input and output categories, respectively. The total of all frequencies is given by *n*.

Table 2. An Example of How to Calculate the Transmitted Information

	1	2	3	4	5
1	20				
2	60	4			
3	20	88	10		
4		8	76	14	
5			12	80	2
6			2	6	8
7					90

The frequencies shown in the table is referred to by means of the symbols given in Table 1, for example, $n_{23} = 88$, $n_{j=2} = 64$, $n_{i=1} = 100$, $n = 500$, and so on.

quantities, namely, $H(x)$, $H(y)$, and $H(x, y)$, can be calculated fromTable 1.

$$H(x) = \sum_i p_i \log_2 \frac{1}{p_i} \tag{7}$$

$$H(y) = \sum_j p_j \log_2 \frac{1}{p_j} \tag{8}$$

$$H(x,y) = \sum_{ij} p_{ij} \log_2 \frac{1}{p_{ij}} \tag{9}$$

where $p_i = n_i/n$, $p_j = n_j/n$, and $p_{ij} = n_{ij}/n$. For simplicity, we can rewrite the above equations as follows:

$$H(x) = \log_2 n - \frac{1}{n} \sum_i n_i \log_2 n_i \tag{10}$$

$$H(y) = \log_2 n - \frac{1}{n} \sum_j n_j \log_2 n_j \tag{11}$$

$$H(x,y) = \log_2 n - \frac{1}{n} \sum_{ij} n_{ij} \log_2 n_{ij} \, . \tag{12}$$

Then, the TI $T(x; y)$ can be obtained from Eq. 3 together with Eqs. 10, 11, and 12. The TI conveys the amount of information that "*y*" has about "*x*."

Table 2 gives an example of how to calculate the TI. Assume that a subject (e.g., a step wedge) having five steps with different thickness was used for the experiment. The five steps correspond to five inputs present equiprobably. The gray-

Table 3. Several Typical Values of Transmitted Information $T(x; y)$ and Conditional Entropy $H_x(y)$ Obtained at the Relative Exposure Doses of 20 and 30 for Three Different Exposure Positions

Step Wedge	Relative Exposure Dose	Position	$T(x; y)$ [bit]	$H_x(y)$ [bit]
		Center	1.72±0.03	6.56±0.04
		Off center, 15 cm	1.61±0.01	6.51±0.01
	20	Off center, 30 cm	1.57±0.01	6.65±0.01
		Center	1.92±0.01	6.37±0.01
		Off center, 15 cm	1.86±0.01	6.24±0.02
A	30	Off center, 30 cm	1.83±0.01	6.25±0.01
		Center	0.76±0.03	6.32±0.01
		Off center, 15 cm	0.60±0.03	6.26±0.01
	20	Off center, 30 cm	0.52±0.01	6.24±0.01
		Center	0.95±0.02	6.04±0.01
		Off center, 15 cm	0.77±0.02	5.90±0.01
B	30	Off center, 30 cm	0.71±0.02	5.96±0.01

Values shown are expressed as mean±standard deviation.

scale pixel values of 100 pixels in each step after imaging were measured randomly. The distributions of the pixel values are considered as the corresponding outputs, and their respective frequencies are given in the table. The frequencies will be referred to by means of the symbols given in the preceding table; for example, n_{12}=60, $n_{j=3}$=118, $n_{i=2}$=100, n=500, and so on. Now, there are three information quantities, namely, $H(x)$, $H(y)$, and $H(x, y)$, that can be calculated directly from the table by using Eqs. 10, 11, and 12 (Table 3).

For the data given in Table 2,

$$H(x) = \log_2 n - \frac{1}{n}\sum_i n_i \log_2 n = \log_2 5 = 2.323$$

(since inputs are equiprobable)

$$H(y) = \log_2 500 - \frac{1}{500}(20\log_2 20 + 64\log_2 64 + 118\log_2 118 \ldots etc.) = 2.575$$

$$H(x,y) = \log_2 500 - \frac{1}{500}(20\log_2 20 + 60\log_2 60 + 4\log_2 4 \ldots etc.) = 3.235$$

Applying Eq. 3 to the values calculated above, we have

$$T(x;y) = H(x) + H(y) - H(x,y) = 2.323 + 2.575 - 3.235 = 1.663.$$

This is the estimate of the amount of information transmitted by the subject from input to output: 1.633 bits, out of a possible of 2.323 bits.

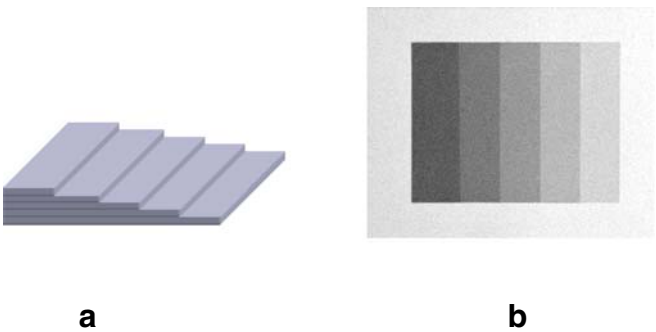

Fig 2. (a) Schematic drawing of an acrylic step wedge. (b) An image obtained from a step wedge used in the study.

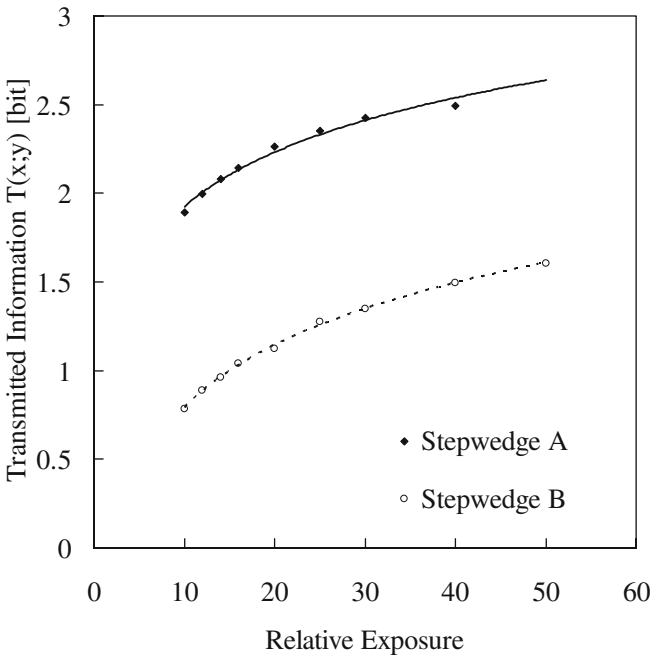

Fig 3. Transmitted information $T(x; y)$ as a function of relative exposure dose for the images obtained from two step wedges. For example, the values of $T(x; y)$ at the relative exposure doses of 20 and 30 for step wedge A are 2.26±0.01 [bit] and 2.44±0.01 [bit], and that for step wedge B are 1.12±0.03 [bit] and 1.35±0.04 [bit], respectively. Values shown are expressed as mean±standard deviation.

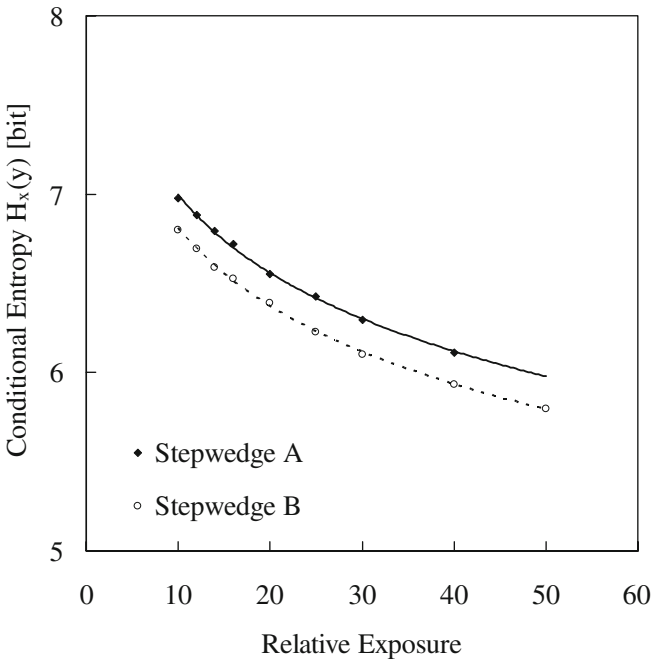

Fig 4. Conditional entropy $H_x(y)$ as a function of relative exposure dose for the images obtained from two step wedges. For example, the values of $H_x(y)$ at the relative exposure doses of 20 and 30 for step wedge A are 6.55±0.01 [bit] and 6.29±0.01[bit], and that for step wedge B are 6.34±0.02 [bit] and 6.10±0.01 [bit], respectively. Values shown are expressed as mean±standard deviation.

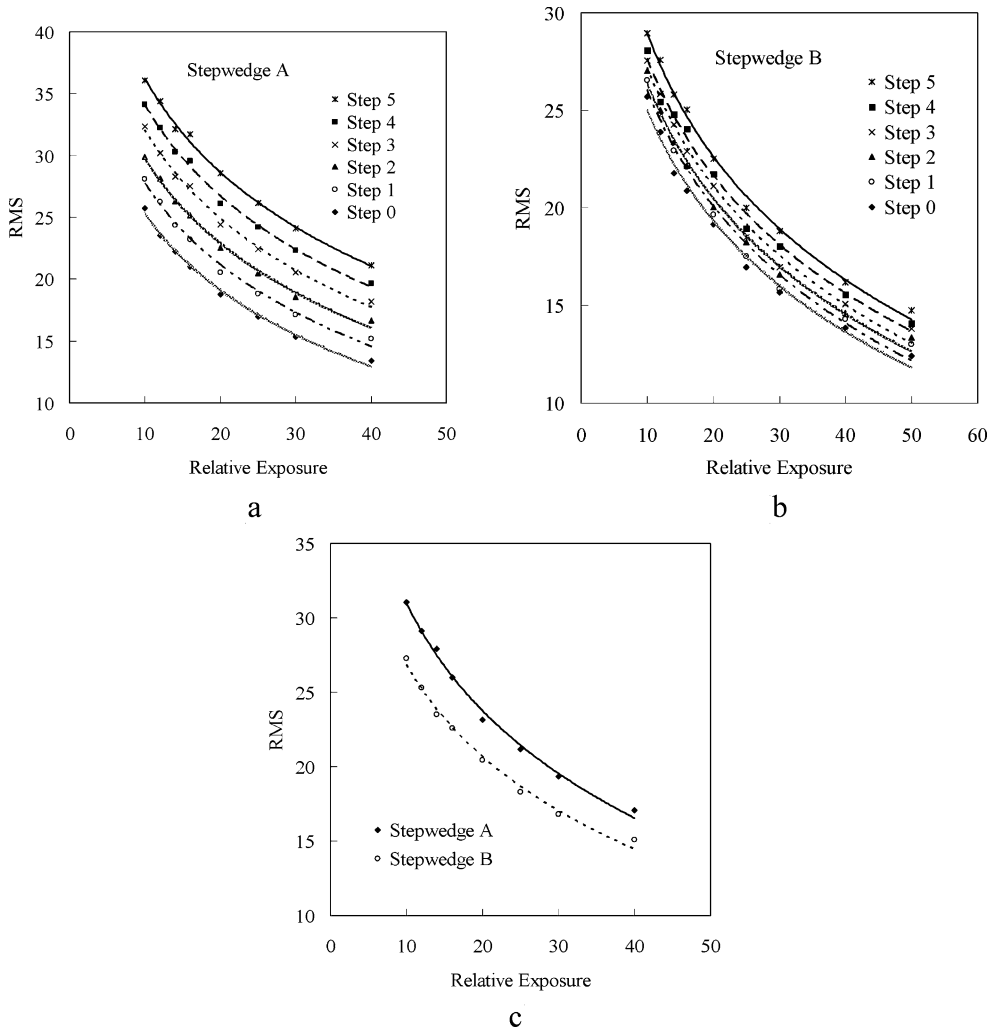

Fig 5. Root-mean-square (RMS) noise as a function of relative exposure dose for the images obtained from two step wedges. (a) RMS for each step (steps 0∼5) of step wedge A, (b) RMS for each step (step 0∼5) of step wedge B, and (c) average RMS obtained by averaging the RMS of various steps. For example, the values of RMS at relative exposure doses of 20 and 30 for step wedge A are 23.17±0.09 and 19.34±0.13, and that for step wedge B are 20.46±0.24 and 16.79±0.17, respectively. Values shown are expressed as mean±standard deviation.

METHODS AND MATERIALS

In the present study, three experiments were made. The first experiment was conducted to verify the effect of noise, the second for analyzing the effect of resolution (blur), and finally, for the third experiment, three filters were used to analyze the combined effect of deteriorated blur and noise on the images.

Two acrylic step wedges with 0–1–2–3–4–5 mm (step wedge A) and 0–2–4–6–8–10 mm (step wedge B) in thickness were prepared as phantoms for the experiments. The specified exposure factors were kept at 42 kV and 10 mA, and the focus-imaging distance was taken as 185 cm, but the exposure time was varied ranging from 0.1 to 0.5 s. An imaging plate for computed radiography was used as a detector to record X-ray intensities. It is clear that when the thickness of the step wedge increases, the intensity of the transmitted X-ray beam is reduced. Therefore, the image consists of a graduated scale of gray levels with different values. Figure 2 shows a schematic drawing of an acrylic step wedge and an image

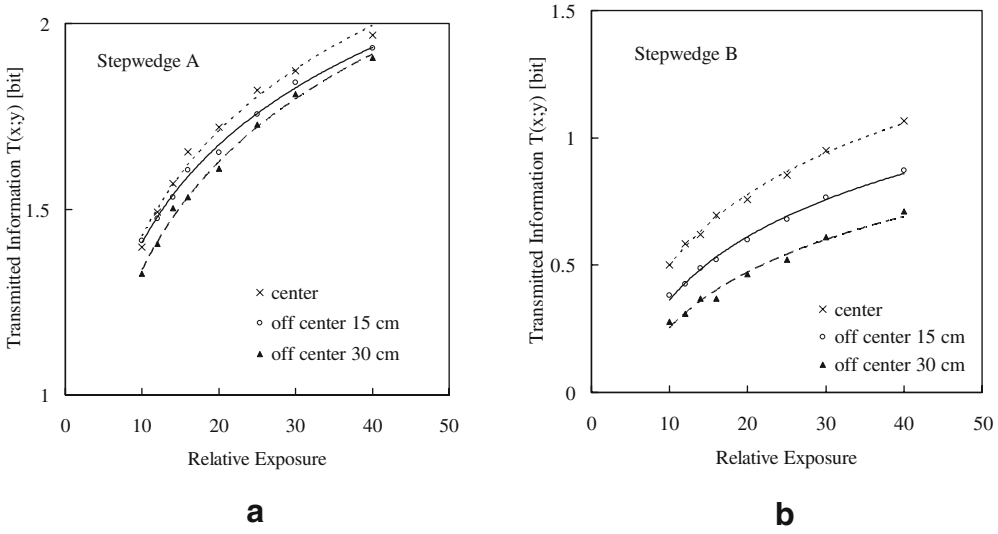

Fig 6. Transmitted information $T(x; y)$ as a function of the relative exposure dose for three different exposure positions to the step wedges: center position of the X-ray beam area, 15 and 30 cm apart from the center toward the cathode end. (a) Step wedge A and (b) step wedge B. Several typical values of the transmitted information are summarized in Table 3.

obtained from a step wedge used in the present study. A region of interest (ROI) located at the center of each step of the step wedge was selected for computation of pixel value distribution. The area of the ROI used in the present study was 100×100 pixels. Therefore, a total of 10,000 data for each step was obtained. Ten images for a particular exposure time were obtained for the present study.

Furthermore, to investigate the relationship between the extent of image blurring and the amount of TI, we changed the effective focal spot sizes of the X-ray tube by shifting the phantoms away from the center of the X-ray beam area toward the cathode end when imaging was performed. Because the effective focal spot size changes and becomes larger for points toward the cathode end of the field,[19] the increase of effective focal spot size

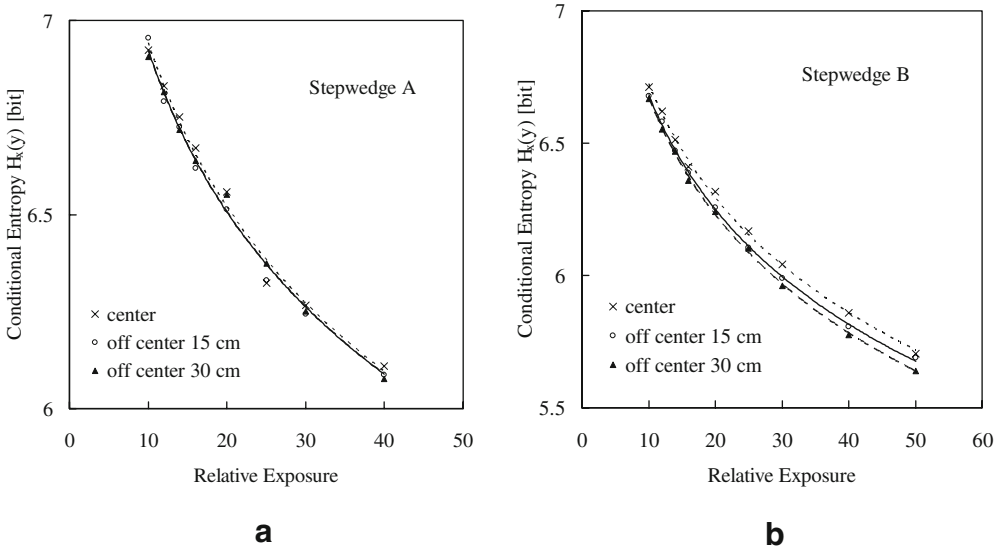

Fig 7. Conditional entropy $H_x(y)$ as a function of the relative exposure dose for three different exposure positions to the step wedges: center position of the X-ray beam area, 15 and 30 cm apart from the center toward the cathode end. (a) Step wedge A and (b) step wedge B. Several typical values of the transmitted information are given in Table 3.

results in the degradation of resolution (blur). To accurately measure the extent of blurring attributed to the change of the effective focal spot size, ROIs having the area of 200×50 pixels located at the boundary of two adjacent steps were selected.

Three commonly used smoothing filters, averaging, median, and Gaussian filters,[20] were employed to analyze the combined effect of blur and noise on the processed images. The images of the step wedges A and B were used as original images. After applying the three filters individually to the step-wedge images, the TI as well as other values related to noise and blur on the processed images were calculated and compared.

RESULTS AND DISCUSSION

Figure 3 shows the relation between the relative exposure dose and TI, $T(x; y)$, for the images of two step wedges. The results illustrate that the $T(x; y)$ increases with the increase of exposure dose. The rise of $T(x; y)$ is considered due to the decrease of noise resulting from the increase of radiation dose. As shown in Figure 4, the value of the conditional entropy $H_x(y)$ decreases when exposure dose increases. A previous study reported by Uchida and Fujita indicated that the $H_x(y)$ is closely related to the noise of an imaging system.[7] The lower the noise level (the higher the exposure dose), the less the $H_x(y)$ value is. Our results well agree with the results of this literature. Figure 5 shows the root-mean-square (RMS) noise. Figure 5a and b presents the RMS value for each step of step wedges A and B as a function of exposure dose, respectively. The average RMS values of the two-step wedges are provided in Figure 5c. It is apparent from the figures that the RMS value decreases with the increase of exposure dose. This result reveals the reasoning that $H_x(y)$ is associated with noise present in an information transmission channel. Thus, it is obvious from the experiments obtained that TI value and the extent of noise are closely correlated.

Figure 6 shows the $T(x; y)$ values obtained by shifting the step wedges 15 and 30 cm away from the center of the X-ray beam area toward the cathode end. The calculated results show that the TI becomes lower when the off-center distance is greater. This means that the TI value decreases when blur is deteriorated. We also compared the RMS noise computed from the step-wedge image without and with shifting from the center. The results showed no significant difference between the two cases (without and with shifting). Similarly, as shown in Figure 7, $H_x(y)$ values obtained from the two cases for the step wedges show insignificant difference. The calculated values of TI and $H_x(y)$ obtained at the relative exposure doses of 20 and 30 for three different exposure positions, are summarized in Table 3. The results imply that the decrease of the TI may be mainly

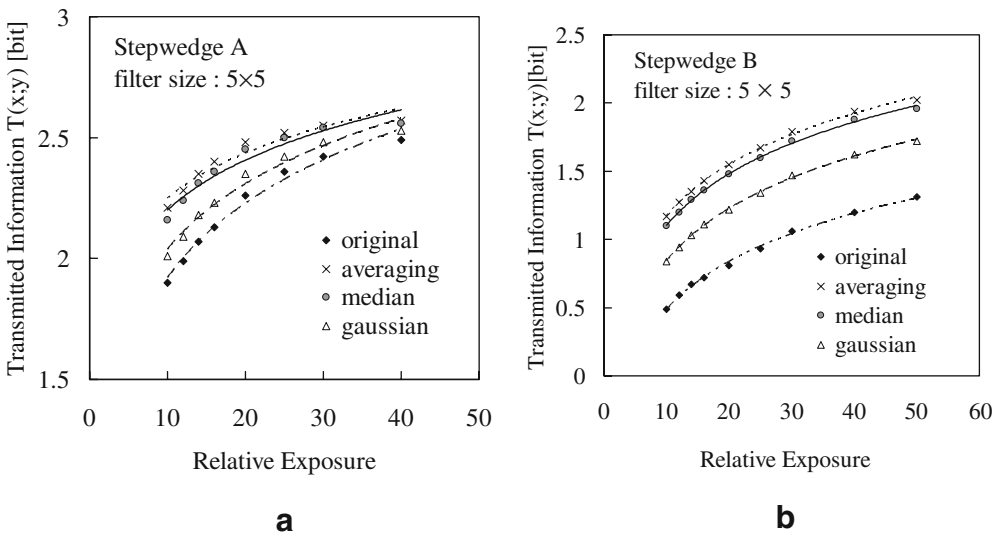

Fig 8. Transmitted information $T(x; y)$ as a function of the relative exposure for the step-wedge images processed by the three filters having a filter size of 5×5. The calculated result of the original image is also shown for comparison. (a) Step wedge A and (b) step wedge B.

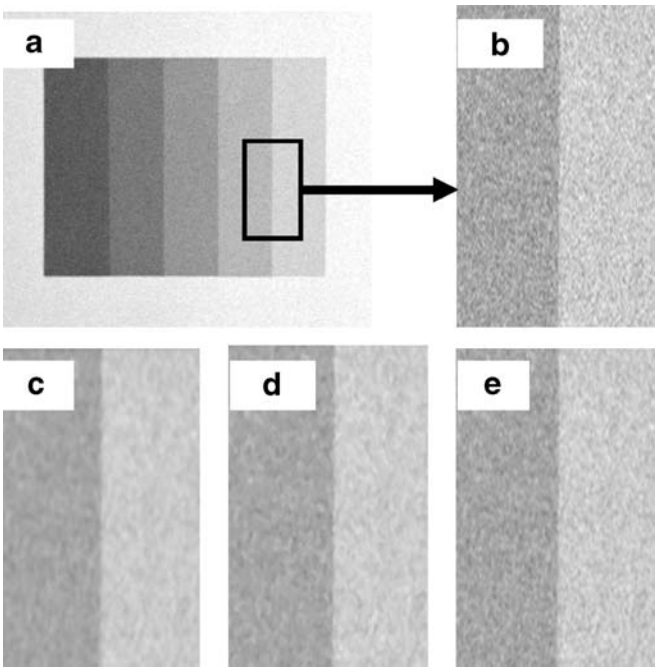

Fig 9. An example of the processed image data. (a) Image of the step wedge used. (b) Magnification of the rectangular area shown in a. (c) Magnified image processed by averaging filter. (d) Magnified image processed by median filter. (e) Magnified image processed by Gaussian filter. To visually differentiate among the three processed images together with the original image, we iteratively performed image processing three times. The calculated results of $T(x; y)$, $H_x(y)$, RMS, and edge slope are summarized in Table 4.

due to image blurring resulting from the increase of the effective focal spot size. Therefore, the TI is also closely correlated with resolution (blur) of imaging systems.

Figure 8 shows the TI as a function of the relative exposure for the step-wedge images processed by the three filters having a filter size of 5×5. The calculated results of the original image are also illustrated for comparison. The experimental results indicate that averaging filter provides the best performance, followed by median and Gaussian filters. Similar performance rankings were obtained when the filter sizes were 3×3 and 7×7. To visually differentiate among the three processed images together with the original image, we iteratively performed image processing three times. Figure 9 shows an example of the processed image data. It can be observed from the figure that image noise level on the three processed images has been reduced, whereas the images were deteriorated and blurred in different extent. Table 4 gives the quantitative comparison among the processed images. It is noted from the table that the averaging filter provides the highest TI, followed by the median and Gaussian filters. In contrast, the averaging filter provides the lowest conditional entropy $H_x(y)$ and RMS noise, followed by the median and Gaussian. Furthermore, we measured the extent of image blurring using an index "edge slope." In this study, the edge slope is defined as the gradient of the mean pixel value profile across the edges of two adjacent steps. The mean profile was obtained by averaging 100 individual ones. As illustrated in the table, the edge slope of the original image is higher as compared with that of the three processed images. The edge slopes of the median and Gaussian filters

Table 4. Values of Transmitted Information $T(x; y)$, Conditional Entropy $H_x(y)$, Noise Level RMS, and Edge Slope for Three Filter-Processed Images and Original Image

Image	$T(x; y)$ [bit]	$H_x(y)$ [bit]	RMS	Edge Slope
Averaging	2.55	5.75	13.2	10.6
Median	2.48	6.03	16.7	14.8
Gaussian	2.26	6.47	21.9	15
Original	1.89	6.97	31.3	17.2

The exposure conditions used to obtain the original images were 42 kV, 10 mA, and 0.1 s.

are almost the same and higher than that of the averaging filter. As a whole, the performance rankings of the three smoothing filters are in the order of averaging, median, and Gaussian. Furthermore, from Figure 9 and Table 4, we note that the perceptual and quantitative results are in good agreement. The results show that the combined effect of deteriorated blur and noise on the images can be analyzed and evaluated using the TI metric.

Our proposed method has limitations. First, an appropriate selection of test object (e.g., step wedges in the present study) is required. In other words, the adjacent pixel value distributions obtained from the input must be partially overlapped (see Table 2). When the pixel value distributions are completely separated, the TI value will exactly equal input entropy $H(x)$. If this case occurs, the proposed metric then can not be used for evaluation of imaging properties. Second, the TI value does not provide frequency information like MTF and NPS do. Also, other noise-contributing properties such as the electronic noise and structural noise cannot be separately represented. A comparison of our proposed metric with MTF and NPS in the same context is needed and is in progress in our ongoing study. Furthermore, this paper did not attempt to conduct the analysis of quantitative influence of image noise and image blurring on the amount of TI. Thus, the extent to which these two factors individually affect the amount of the TI still remains unclear. We will investigate this issue in our future research.

CONCLUSIONS

In this work, we presented a metric using TI for measurement of physical image quality. Our experimental results showed that the amount of TI is correlated with both image noise and image blurring. The results indicate the potential usefulness of the proposed method for evaluation of physical image quality.

ACKNOWLEDGMENT

The authors would like to thank Mr. Yoshihiko Watanabe of Niigata University for his assistance in the experiments.

REFERENCES

1. Dobbins III JT: Effect of undersampling on the proper interpretation of modulation transfer function, noise power spectra, and noise equivalent quanta of digital imaging systems. Med Phys 22:171–181, 1995

2. Kyprianou IS, Rudin S, Bednarek DR, Hoffmann KR: Generalizing the MTF and DQE to include X-ray scatter and focal spot unsharpness: Application to a new microangiographic system. Med Phys 32:613–626, 2005

3. Shannon CE: A mathematical theory of communication. Bell Syst Tech J 27:379–423/623–656, 1948

4. Shannon CE, Weaver W: The mathematical Theory of Communication. University of Illinois Press, Urbana, 1949

5. Uchida S, Tsai DY: Evaluation of radiographic images by entropy: Application to development process. Jpn J Appl Phys 17:2029–2034, 1978

6. Uchida S, Tsai DY: Reliability of the modulation transfer function of radiographic screen-film system measured by the slit method. Jpn J Appl Phys 18:1571–1574, 1979

7. Uchida S, Fujita H: Assessment of radiographic granularity by a single number. Jpn J Appl Phys 19:1403–1410, 1980

8. Kim B, Boes JL, Frey KA, et al: Mutual information for automated unwarping of rate brain autoradiographs. Neuroimage 5:31–40, 1997

9. Studholme C, Hill DLG, Hawkes DJ: An overlap invariant entropy measure of 3D medical image alignment. Pattern Recog 32:71–86, 1999

10. Hayton PM, Brady M, Smith SM, et al: A non-rigid registration algorithm for dynamic breast MR images. Artif Intell 114:125–156, 1999

11. Bruckner T, Lucht R, Brix G: Comparison of rigid and elastic matching of dynamic magnetic resonance mammographic images by mutual information. Med Phys 27:2456–2461, 2000

12. Thurfjll L, Lau YH, Andersson JLR, et al: Improved efficiency for MRI-SPET registration based on mutual information. Eur J Nucl Med 27:847–856, 2000

13. Skouson MB, Guo Q, Liang ZP: A bound on mutual information for image registration. IEEE Trans Med Imag 20:843–846, 2001

14. Shekhar Rand, Zagrodsky V: Mutual information-based rigid and nonrigid registration of ultrasound volumes. IEEE Trans Med Imag 21:9–22, 2002

15. Qu G, Zhang D, Yan P: Information measure for performance of image fusion. Electron Lett 38:313–315, 2002

16. Pluim JPW, Maintz JBA, Viergever MZ: Mutual-information-based registration of medical images: A survey. IEEE Trans Med Imag 22:986–1004, 2003

17. Filev P, Hadjiiski L, Shiner B, et al: Comparison of similarity measures for the task of template matching of masses on serial mammograms. Med Phys 32:515–529, 2005

18. Attneave F: Applications of Information Theory to Psychology. New York: Holt, Rinehart and Winston, 1959

19. Sprawls P: Physical Principles of Medical Imaging. Madison, WI: Medical Physics Publishing, 1995, pp 273–274

20. Russ JC: The Image Processing Handbook, 2nd edition. London: CRC, 1995